

5 APPLICATION OF A LARGE-SCALE WATER BALANCE MODEL TO THE TANA RIVER BASIN

5.1 Introduction

Conceptual water balance models are often believed to be useful in assessing the impact of climatic changes on regional hydrology, and have successfully been applied at larger scales (Arnell, 1999; Kwadijk, 1993). In terms of data demands, accuracy, flexibility and ease of use they have significant advantages over lumped empirical models or physically-based models (Xu, 1999). Most models currently in use have been developed for temperate climatic conditions. However, sub-arctic environments, such as the Tana Basin in Northern Fennoscandia (see chapter 2), are very distinct in their hydrological behaviour. The water balance of these areas is dominated by a long-lasting snow cover in winter, while in summer evapotranspiration may predominate in many areas (Mackay & Løken, 1974; Rovensek et al., 1996; see also chapter 3). Moreover, many models are designed to simulate river discharge, and may not be able to simulate spatial patterns in snow coverage or evaporation realistically. The objective of this chapter is therefore to explore the performance of a GIS-based water balance model, developed for the Rhine, in the sub-arctic Tana Basin. This model, named RHINEFLOW (Kwadijk, 1993), was applied to the Tana Basin without significant changes in the model concept. The data that were used and the assumptions that had to be made, are discussed in this chapter. In evaluating the model performance, attention is paid those processes that dominate the water balance of this area. Finally, some suggestions for model improvement are given.

5.2 The concept of water balance

The water balance of an area describes the relation between input, storage and output of water. While input in the form of precipitation is mainly dependent on climate, the output, either in the form of river discharge or evapotranspiration, also depends on vegetation and catchment characteristics. In the longer term, i.e. on a yearly basis or longer, changes in storage can usually be neglected, and the water balance can be written as:

$$Q = P - E \quad (5.1)$$

where Q = river discharge
 P = amount of precipitation
 E = amount of evapotranspiration

According to Woo (1990), however, year-to-year changes in water storage may not be negligible in (non-glacial) permafrost basins. Theoretically the annual partitioning of precipitation into evapotranspiration and runoff is controlled by the temporal distribution

of water supply (precipitation) and demand (evapotranspiration), which are balanced by water storage in the soil (Milly, 1994). At smaller than annual time scales – monthly, daily or even hourly – the changes in and interactions between the storages that can be identified in a catchment, have to be taken into account:

$$Q = P - E \pm \Delta S \quad (5.2)$$

where ΔS = change in storage

These storages include water storage in vegetation, surface detention, storage in snow and glaciers, soil storage, groundwater storage, and storage in lakes and channels (Kwadijk, 1993). The importance of each component differs in time and in space. In sub-arctic catchments for example, storage of precipitation in snow is much more important than in temperate environments.

5.3 Water balance of the Tana Basin

Annual water balance characteristics of the Tana Basin (chapter 2) were analysed for a period of 20 years: October 1979 through September 1999 (referred to as 1980-1999). For this purpose, daily temperature and precipitation data from the meteorological stations listed in table 5.1 were extrapolated to the entire river basin using Thiessen polygons. Mean annual precipitation in this period amounted to 401 mm, and the mean annual temperature was -2.0°C . The second half of this period (1990-1999) was considerably warmer than in the first (-1.51°C vs. -2.50°C in 1980-1989). The second half also received slightly more precipitation (405 vs. 398 mm/year). Due to the large interannual variability, a significantly drier or wetter period could not be identified.

A first indication of the water balance was obtained by comparing the basin-averaged precipitation with observations on river runoff. The ratio of observed discharge and precipitation (Q/P ratio) in the Tana basin and several subcatchments is given in table 5.2. Obviously, these ratios are too high. Considering the fact that a significant proportion of the annual rainfall in the area is lost to evapotranspiration, the average Q/P ratio should be less than 1.0. However, in several subbasins it is even higher than 1.0, which is theoretically impossible. According to equation (5.1), the difference between input (P) and output (Q) indicates the amount of evapotranspiration (E) in the entire basin. Upstream of Polmak, Norway, this difference is only 3 mm/year in the period 1980-1989. This estimate is not realistic. As demonstrated in chapter 3, the actual amount of evapotranspiration in this area is much higher.

There are two possible explanations for the unrealistic Q/P ratios in table 5.2: the observed discharge of the Tana River is too high, or the precipitation measurements are too low. Most precipitation stations are located in the river valleys (see figure 5.1), and may not be representative for the surrounding upland areas, that constitute the greatest part of the Tana Basin. Moreover, it is a well-known problem that precipitation gauges

Table 5.1 Meteorological stations in the Tana Basin used in this chapter, and their observation period of temperature and precipitation between October 1979 and September 1999. For locations, see figure 5.1

	Precipitation	Temperature
Rustefjelbma	10/79 – 9/99	10/79 – 9/99
Kevo	10/79 – 9/99	10/79 – 9/99
Karasjok	10/79 – 9/99	10/79 – 9/99
Cuovddatmohkki	10/79 – 9/99	10/79 – 9/99
Sihcajavri	10/79 – 9/99	10/79 – 9/99
Polmak, Polmak II	10/79 – 7/98	
Sirbma	10/79 – 9/99	
Skoganvarre	10/79 – 12/79	
Port	8/81 – 9/99	
Valjok	10/79 – 9/99	
Iskorajohka	10/79 – 9/99	
Jergol	8/81 – 9/99	
Mollesjohka	10/79 – 9/99	
Jotkajavre	10/79 – 9/99	

systematically underestimate snowfalls (Goodison et al., 1998; Yang et al., 2001). In addition, point snow data are not representative for the snow cover of an area (Yang & Woo, 1999). Assuming that the discharge measurements are correct, it appears that precipitation in the catchment area is seriously underestimated by direct extrapolation of the observations.

5.4 Model description

In a previous study, Kwadijk (1993) developed a water balance model of the Rhine Basin, and used it to study the impact of climate change on the discharge of the River Rhine. This model, named RHINEFLOW, is a GIS-based, conceptual water balance model that uses standard meteorological input variables, and geographical data on topography, land cover, soil type and groundwater flow characteristics. Parameters and variables are stored in a raster Geographical Information System (GIS) called PCRaster, and the model itself is implemented in PCRaster using a scripting language (Van Deursen, 1995). Considering its limited data demands and ease of use, this model was applied to the Tana River Basin. A brief introduction to the concept of the model is given in this section.

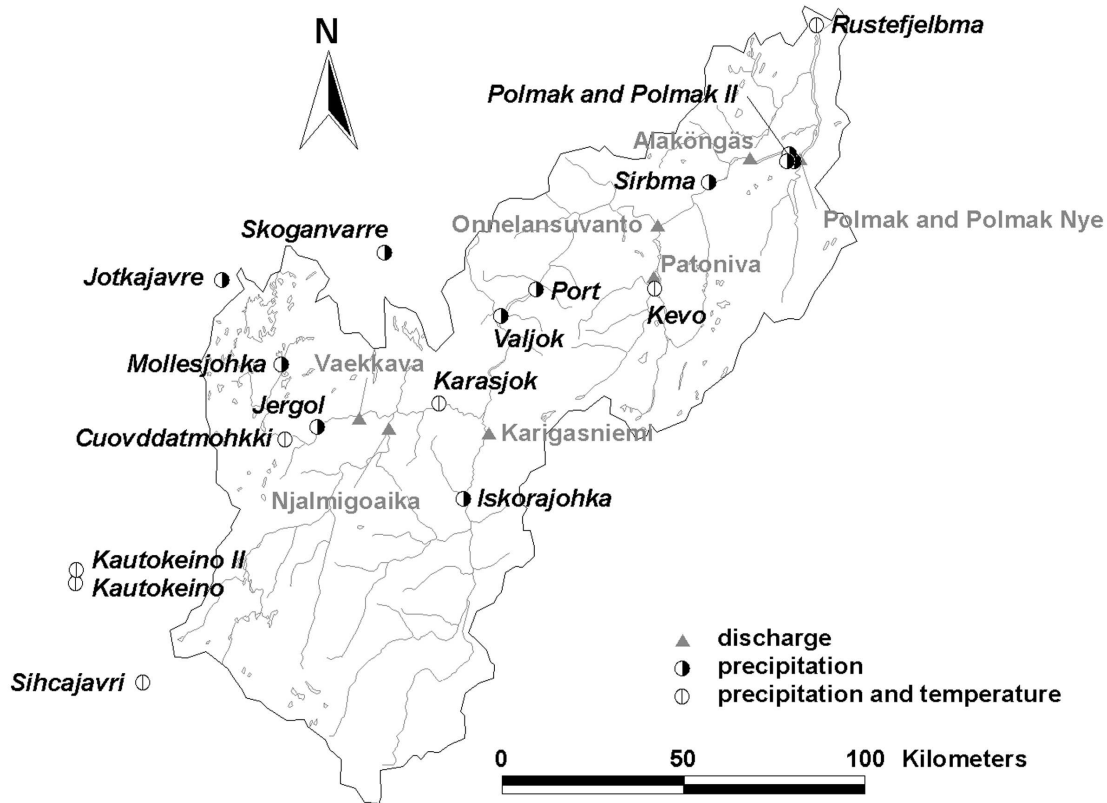


Figure 5.1 Location of meteorological stations and discharge stations in the Tana Basin

5.4.1 Model concept

Following the water balance equation (5.2), RHINEFLOW calculates runoff as a function of precipitation, actual evapotranspiration and changes in water storage. The model identifies four storages: snow, soil, groundwater and lakes. For each time step the input, storages and losses are calculated for each cell, and the produced discharge is accumulated over a digital elevation model (DEM) of the catchment to determine runoff at the outflow point (figure 5.2). A hydraulic routing scheme, that calculates travel times of runoff, is not included in the model. The water balance calculations of RHINEFLOW are based on the concept of Thornthwaite & Mather (1957). This approach takes possible soil water deficiencies into account when calculating actual evapotranspiration. Snow accumulation and snowmelt are simulated using the temperature-index method; discharge is a combination of rapid runoff (a fraction of the water surplus of the soil compartment) and baseflow from the groundwater store. Originally designed for monthly timesteps and grid cells of 3 by 3 km, the model has later been applied to the Rhine Basin at 1 by 1 km cells with 10-day timesteps (Van Deursen, 1999^a). The main components of the model are described below.

Table 5.2 Runoff / rainfall (Q/P) ratios of observed runoff for the Tana Basin and several sub-catchments in the period 1980-1999. For locations, see figure 5.1

Discharge station	River	Q/P ratio		
		1980-1989	1990-1999	1980-1999
Vækkava	Jiesjåkka	0.93		
Njalmigoaika	Karasjåkka	0.94		
Karigasniemi	Inarijoki	1.06	0.95	1.01
Patoniva	Utsjoki	0.97	0.99	0.98
Onnelansuvanto	Tana (Tenojoki)	1.12	1.03	1.07
Alaköngäs	Tana (Tenojoki)	1.10	1.03	1.06
Polmak	Tana	0.95		

5.4.2 Snow storage and melt

Similar to many other hydrological models, such as the Snowmelt Runoff Model (SRM) (Martinec et al., 1994) and the HBV model (Bergström, 1995), RHINEFLOW uses a temperature-index approach to estimate snow accumulation and melt. In this approach a degree-day factor (DDF) is used to convert air temperature above a certain threshold to snowmelt in mm (Ferguson, 1999):

$$M = (T_a - T_0) \times DDF \quad (5.3)$$

where M = amount of snowmelt (mm.month⁻¹)
 T_a = air temperature (°C)
 T_0 = threshold temperature (°C)
 DDF = degree-day factor (mm.°C⁻¹.month⁻¹)

The degree-day coefficient implicitly represents all terms of the energy budget that account for the mass balance of a snow pack, and is therefore highly variable over time (Melloh, 1999). For this reason, several models allow the DDF to vary in time, instead of using a constant value. Martinec et al. (1994) recommend to increase the DDF twice a month, to account for lower albedo, higher aerodynamic roughness and higher liquid water content as the snowpack ages. In the HBV model season- and weather-dependent degree-day factors were tested, but without much success (Lindström et al., 1997). The melt rate may also differ between vegetation types. Wind speed and turbulent heat transfer in forests for example are generally lower than in open areas. Several models such as HBV and the Semi-distributed Land Use-based Runoff Processes (SLURP) model (Kite, 1995) have therefore been applied with different snowmelt rates for several

land use classes (see e.g. Kite & Kouwen, 1992). In the latest version of RHINEFLOW (Van Deursen, 1999^a), minimum and maximum temperatures, instead of the mean temperature, may be used to calculate snowmelt. In this case snowfall is triggered by the minimum temperature, and the fraction of precipitation falling as snow is equal to the fraction of the temperature interval between minimum and maximum temperature that is below the snowfall-threshold temperature. Likewise, snowmelt is triggered by the maximum temperature, but decreased for the fraction of the temperature interval that is below the snowmelt-threshold temperature.

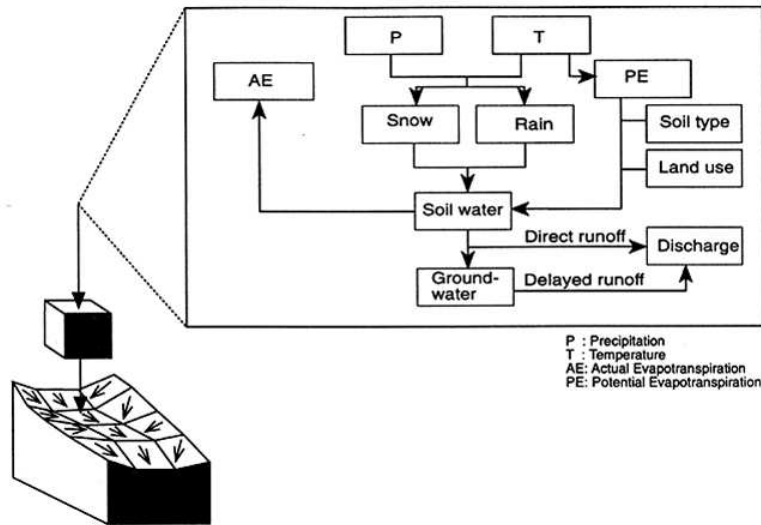


Figure 5.2 Flowchart of RHINEFLOW (after Kwadijk, 1993)

In many areas the temperature-index method may perform well but it is dependent on an appropriate degree-day factor (*DDF*). This factor can be determined by field experiments, or will have to be obtained by calibration otherwise. Singh et al. (2000) list several *DDF*s reported by researchers, ranging from 1.3 to 8.0 mm.°C⁻¹.day⁻¹ for snow and from 5.0 to 13.8 mm.°C⁻¹.day⁻¹ for ice. Kwadijk (1993) used a much lower value of 18 mm.°C⁻¹.month⁻¹ for the Alpine regions of the Rhine basin. Kite & Kouwen (1992) used different factors for different land use classes, ranging from 1.04 mm.°C⁻¹.month⁻¹ for bare soil to 3.78 mm.°C⁻¹.day⁻¹ for forested areas.

5.4.3 Evapotranspiration

The Thornthwaite method of estimating potential evapotranspiration (E_p) (Thornthwaite & Mather, 1955; 1957) is based on air temperature and day length only. Expressed on a monthly basis it reads (Ward & Robinson, 1990; Sellinger, 1996):

$$E_{pi} = 16 \times d_i \left(\frac{10T_i}{I} \right)^a \quad (5.4)$$

where E_{pi} = potential evapotranspiration in month i (mm.month⁻¹)
 d_i = day length correction factor (Rosenberg et al., 1983):

$$d_i = \left(\frac{L_i}{12} \right) \times \left(\frac{N_i}{30} \right) \quad (5.5)$$

L_i = mean actual day length (h)
 N_i = number of days in the month under consideration
 T_i = mean air temperature (°C)
 I = heat index, which is a summation of the monthly heat indexes:

$$I = \sum_{i=1}^{12} \left(\frac{T_i}{5} \right)^{1.514} \quad (5.6)$$

a = a cubic function of I , namely:

$$a = 0.49 + 0.179 I + 7.71 \times 10^{-5} I^2 + 6.75 \times 10^{-7} I^3 \quad (5.7)$$

Thornthwaite & Mather (1957) recommend to use the day length correction factors of 50° N also for higher latitudes.

The Thornthwaite method requires only temperature and hours of daylight, and these two variables are relatively easy to obtain. Consequently, it has been applied in many studies in a wide range of climatological conditions, often with reliable results (Penman, 1956; Pereira & Camargo, 1989). Less good results can be expected over very short periods of time (when mean temperature is not a suitable measure of incoming radiation) and in environments with rapidly changing air temperature and humidity resulting from advection effects, such as the British Isles (Ward & Robinson, 1990). According to Rosenberg et al. (1983) E_p is likely to be underestimated at the time of annual maximum radiation reception during summer.

In RHINEFLOW the potential evapotranspiration is modified with a crop factor to obtain potential evapotranspiration rates for different land use types (Kwadijk, 1993). If the combined input of precipitation and snowmelt exceeds this potential evapotranspiration, the actual evapotranspiration is assumed to be equal to the latter. Otherwise, the actual evapotranspiration is a combination of the available precipitation and a change in soil moisture:

$$\begin{aligned}
E_{ai} &= E_{pi} && \text{if } (P_i + M_i) \geq E_{pi} \\
E_{ai} &= P_i + M_i + (SM_{i-1} - SM_i) && \text{if } (P_i + M_i) < E_{pi}
\end{aligned} \tag{5.8}$$

where E_{ai} = actual evapotranspiration in month i (mm.month⁻¹)
 P_i = amount of rain (mm)
 SM_i = amount of water stored in the soil (mm)

Instead of calculating evapotranspiration rates with the Thornthwaite method, Van Deursen (1999^a) used reference crop evapotranspiration data as input data in RHINEFLOW. In climate change studies, an empirically derived relationship between temperature change and reference evaporation change was used to estimate changes in evaporation.

Since the Thornthwaite method was developed for temperate environments in the USA, the performance in the sub-arctic Tana basin was tested separately. Figure 5.3 shows the Penman-based evapotranspiration estimations for the Kidisjoki catchment near Kevo, Finland (see chapter 3). Also shown are potential evaporation estimates based on the Thornthwaite method, using day length correction factors of this specific site (equation 5.5), as well as those for 50° N, as recommended by Thornthwaite & Mather (1957). As can be seen the Thornthwaite-based estimates of potential evapotranspiration are much higher than those predicted by Penman-Monteith. According to the latter the overall evaporation in the period 22 June – 2 August 1999 is 74 mm or 1.8 mm/day, which corresponds to flux measurements in the same area (chapter 3). The Thornthwaite estimates amount to 5.2 mm/day using local day length correction factors, and 3.5 mm/day using the correction of 50° N. If no day length correction is applied at all, the evaporation estimate is still 2.7 mm/day. Assuming that the estimates of Penman-Monteith – being one of the most advanced evapotranspiration models currently available (Shuttleworth, 1993) – are correct, the Thornthwaite model appears to overestimate evaporation in this sub-arctic environment considerably.

5.4.4 Soil and groundwater storage

Soil moisture is calculated as a function of the maximum water holding capacity of the soil and the accumulated potential water loss:

$$\begin{aligned}
SM_i &= MWC \times e^{(-APWL_i / MWC)} \\
APWL_i &= APWL_{i-1} - (P_i + M_i) + E_{pi} && \text{if } (P_i + M_i) < E_{pi}
\end{aligned} \tag{5.9}$$

where MWC = maximum water holding capacity (mm)
 $APWL_i$ = accumulated potential water loss (mm)

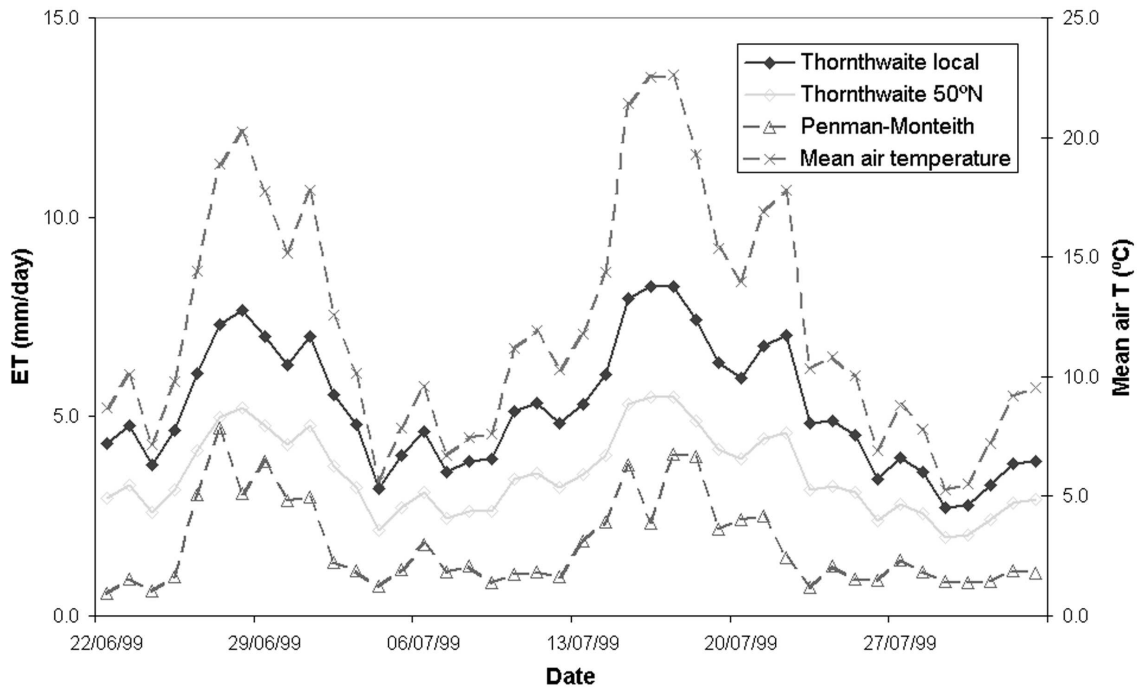


Figure 5.3 Evapotranspiration estimates for the Kidisjoki catchment near Kevo, Finland, in the summer of 1999, based on Penman-Monteith (see chapter 3), and based on the Thornthwaite method using both local and 50°N day length correction factors. Also shown is the temperature course in the study period

Any water surplus (i.e. $SM_i > MWC$) is separated into rapid runoff, that contributes to the discharge of the month under consideration, and a volume of water that is added to the groundwater reservoir. This is controlled by a separation ratio χ that has to be obtained by calibration:

$$\chi = \frac{Q_r}{Q_{gw} + Q_r} \quad (5.10)$$

where Q_r = rapid runoff ($\text{mm} \cdot \text{month}^{-1}$)
 Q_{gw} = amount of water added to groundwater ($\text{mm} \cdot \text{month}^{-1}$)

In the Rhine Basin, Kwadijk (1993) found a value for χ of 0.2, meaning that 20% of the water surplus from the soil compartment is discharged directly as rapid runoff, and 80% is drained to the groundwater reservoir. Baseflow from the groundwater reservoir is calculated with a recession equation:

$$Q_b = \frac{GWS}{C} \quad (5.11)$$

where Q_b = baseflow (mm.month⁻¹)
 GWS = amount of water stored as groundwater (mm)
 C = recession parameter (months)

The recession parameter was calibrated for the main tributaries of the Rhine, using observed discharges of low flow months. According to Kwadijk (1993) low values of C and high values of the separation ratio χ represent catchments with a short response time (relatively steep hydrographs), while high values of C and low values of χ represent a long response time (relatively flat hydrographs). Kwadijk also assumed that C is mainly dependent on the geohydrological properties of a catchment and will not change under changing climatic conditions. By calibrating on discharge data the recession parameter is however dependent on present reservoir storage, which may not correspond with the catchment storage capacity. The latter is mainly dependent on the dimensions and lithological characteristics of the catchment. The ratio of present reservoir storage to the catchment storage capacity is an indication of the sensitivity of the catchment to climate variability or change (Van der Wateren – de Hoog, 1997).

5.5 Application to the Tana Basin

In order to test its performance in a sub-arctic environment, the RHINEFLOW model of Kwadijk (1993), that is described in the previous section, was applied to the Tana River Basin in Northern Fennoscandia. The model was consequently called TANAFLOW, and was applied on a 10-day basis, without further modifications to the model concept. This section describes the input data that were used, the procedure that was followed, as well as the performance of the model.

5.5.1 Modelling period

The model was applied to the period October 1979 – September 1999 (or 1980-1999, see section 5.3). Each month in this period was divided into three parts: the first and second period of 10 days, and the remaining period of 8, 9, 10 or 11 days. The dataset was furthermore split into two equal parts, the first half (1980-1989) was used for calibration and second half (1990-1999) for validation of the model. Before each model run, the calculations of the first 5 years were repeated, in order to reduce initialisation effects.

5.5.2 Input data

The data that were used in the application of the model to the Tana Basin, are listed below. All spatial data were stored as raster maps with a resolution of 1 by 1 km.

- *Precipitation and temperature*
Data on precipitation and temperature were interpolated from the meteorological stations listed in table 5.1 with Thiessen polygons, as in section 5.3. Meteorological observations were however not continuous for all stations used and even within the periods of observation some missing data occurred. The spatial interpolation of the meteorological data was therefore incorporated in the dynamic section of the model. This means that the interpolation with Thiessen polygons was repeated in each time step, using only those stations for which data were available. Temperature values were corrected for elevation differences using a DEM of the Tana Basin, assuming a 0.57°C temperature decrease per 100 m elevation increase.
- *Thornthwaite coefficients*
The annual heat index I and coefficient a (equations 5.6 and 5.7) were calculated for each temperature station that was used in the model run (table 5.3). The evapotranspiration estimates were corrected for day length, which was calculated for each station using software from Lammi (2001).

As discussed in section 5.4.3, estimates of evapotranspiration based on the Thornthwaite method are too high in sub-arctic environments. The Thornthwaite estimates were therefore adjusted to meet the long-term water balance the Tana Basin (see section 5.3). In 1980-1999, the ratio of observed runoff and observed (basin-averaged) precipitation ranged between 0.95 and 1.12 (table 5.2). To obtain a similar ratio of simulated runoff and rainfall, the evapotranspiration estimates of the model need to be scaled by a factor 0.01 – 0.03 (table 5.4). However, in section 5.3 it was argued that the Q/P ratios in table 5.2 are too high, and that the observations at the meteorological stations underestimate precipitation over the entire catchment area. In other words, a Q/P ratio of 0.95 does not reflect the actual proportion between rainfall and runoff in the catchment. As an alternative, a reduction factor of 0.1 resulted in a lower runoff / precipitation ratio of 0.88 (see table 5.4), and appeared to yield slightly higher

Table 5.3 Annual heat index (I) and Thornthwaite coefficient a for temperature stations in the Tana Basin, calculated for the period 1980-1999

	I	a
Rustefjelbma	9.84	0.66
Kevo	11.26	0.68
Karasjok	12.16	0.70
Cuovddatmohkki	10.60	0.67
Sihcajavri	11.25	0.68

modelling efficiencies as well. It was therefore decided to apply this scaling factor to the modelled evapotranspiration rates.

- *Digital Elevation Model (DEM)*

A digital elevation model (DEM) of the Tana Basin was obtained from the GTOPO30 data set of the US Geological Survey's EROS Data Centre. This data set provides elevation data with a nominal cell size of 1 km, and is derived from various vector and raster data sets. The vertical accuracy varies by location according to the source data; for the Tana basin an accuracy of ± 30 m at the 90 % confidence level is indicated (Defense Mapping Agency, 1986). This corresponds with a root mean square error of 18 m, assuming that the errors show a Gaussian distribution with a mean of zero (US Geological Survey, 2000). The catchment of the Tana river was delineated following a procedure outlined by Wesseling et al. (1997).

- *Vegetation map*

A Landsat TM satellite image of 18 July 1987 was used to map vegetation types in the Tana Basin (see section 2.3.3 and figure 2.5). This map was converted into crop factors, that were used in the calculation of evapotranspiration rates for each specific land cover type. Unfortunately, no crop factors have been published for the specific vegetation types occurring in the Tana basin. The crop factors that were used are therefore based on comparable vegetation types in the Rhine Basin, as published by Brechtel & Scheele (1982) (see table 5.5).

- *Soil map*

According to the FAO-UNESCO soil map of the world (Zobler, 1986) medium coarse soils (orthic podsols, texture class sandy loam) and organic soils

Table 5.4 Simulated runoff / rainfall (Q/P) ratios with several adjustments of the evapotranspiration estimates

Day length correction factor	Evaporation reduction factor	Q/P ratio
-	1	0.39
50°N	1	0.27
Local	1	0.15
Local	0.5	0.47
Local	0.1	0.88
Local	0.05	0.93
Local	0.03	0.95
Local	0.01	0.97

predominate in Northern Fennoscandia. This dataset has a spatial resolution of only 1 by 1 degree latitude / longitude. Quarternary geology maps of the area (e.g. Olsen et al., 1996) show much more detail, and indicate that most of the Tana Basin is covered by glacial till, except for open water, wetlands and those areas where bedrock is exposed. The vegetation map was therefore used as a basis for the soil map, by re-labelling the vegetation classes into soil types according to table 5.5.

The maximum soil water capacity of the glacial till was estimated based on published data from Bouwman et al. (1993) and Vörösmarty et al. (1989). According to the latter the saturation capacity of sandy loam is 41.3 %, and for silty loam (medium, coarse-fine and coarse-medium-fine) 46.8 %. The actual amount of water that can be stored is furthermore dependent on rooting depth. Observations on rooting depth were made in the Kidisjoki catchment near Kevo, Finland (see chapter 3). Here, rooting depth at non-forested sites (such as alpine heaths) was in general not more than 20 cm, and soil development usually did not reach below 30 cm depth. The saturation capacity of non-forested sites with a sandy loam texture may therefore be estimated at $(41.3\% \times 200 =)$ 83 mm, assuming a root depth of 20 cm, or 124 mm based on 30 cm soil development. For silty loam these values are 94 and 140 mm respectively. In forested and semi-forested areas the maximum soil water capacities can expected to be higher because of the larger rooting depth. As an average, the maximum soil water capacity of all areas (both forested and non-forested) consisting of glacial tills was therefore estimated at 150 mm. As argued in chapter 3, the storage capacity of arctic wetlands may be limited (see also Quinton & Roulet, 1998), and a much lower value was therefore chosen for this land cover type. The maximum soil water holding capacity of bare rock is based on Groenendijk (1989). To allow for temporary storage of water in lakes by fluctuations in the water table, a storage capacity of 10 mm was assumed.

Table 5.5 Recoding of vegetation types in the Tana Basin into crop factors, soil types and maximum soil water capacities (*MWC*)

	Crop factor	Soil type	<i>MWC</i> mm
Lakes	1.0	Water	10
Wetland	1.0	Peat	10
Sand / gravel, bare rock, boulder fields	0.4	Bare rock	30
Birch forests (high density), pine forests	1.1	Glacial till	150
Alpine heaths, meadows, birch forests (low density)	0.9	Glacial till	150

5.5.3 Calibration

The model was calibrated using observed discharge at several stations in the Tana Basin (table 5.6). The calibration was carried out by adjusting the values of the degree-day factor (*DDF*) for snowmelt, the separation ratio (χ) of quick runoff and groundwater flow, and the recession parameter (*C*) for baseflow calculation. As calibration procedure a “brute force” Monte Carlo technique was used, meaning that all possible combinations of *DDF*, χ , and *C* were calculated, within a given range of parameter values and with fixed increments. The results were compared with the observed discharge for all locations, and several error statistics were calculated: the Nash & Sutcliffe (1970) coefficient of efficiency, the mean bias error (Barr et al., 1997), the mean difference between measurement and simulation (Addiscott et al., 1995) and the product moment-correlation (*r*) (Addiscott et al., 1995).

The most downstream discharge gauging station available is Polmak, Norway. In terms of the Nash-Sutcliffe coefficient the best results for this station were obtained with the following parameter combination: *DDF* = 14 mm.°C⁻¹ per 10-day period, χ = 0.7 and *C* = 30 10-day periods (figure 5.4). In the Rhine basin these values were 18 mm.°C⁻¹ per month, 0.20 and 1 to 6 months respectively (Kwadijk, 1993). The higher value of χ indicates a much shorter response time of the Tana basin (section 5.4.4), while the higher *DDF* may represent the high snowmelt rates in the Tana Basin. The Nash-Sutcliffe coefficient of this parameter set is 0.59 in the calibration period 1980-1989, and the product-moment correlation (*r*) is 0.77. In the various sub-basins different parameter combination give the best results (see table 5.7). It is interesting to note that in the smaller subcatchments the best results were obtained with higher *DDF* values of about 20 mm.°C⁻¹.period⁻¹, except for the Jiesjåkka river in Norway.

Table 5.6 Discharge stations used in the calibration of TANAFLOW, and period of observation. For locations, see figure 5.1

Discharge station	River	Catchment size km ²	Period of observation
Polmak	Tana	14386	1911 - 1992
Polmak Nye	Tana	13601	1991 - 1994
Alaköngäs	Tana (Tenojoki)	13457	1963 - present
Onnelansuvanto	Tana (Tenojoki)	10505	1959 - present
Patoniva	Utsjoki	1458	1963 - present
Karigasniemi	Inarijoki	2868	1961 - present
Vækkava	Jiesjåkka	2071	1973 - 1995
Njalmigoaika	Karasjåkka	2264	1966 – 1991

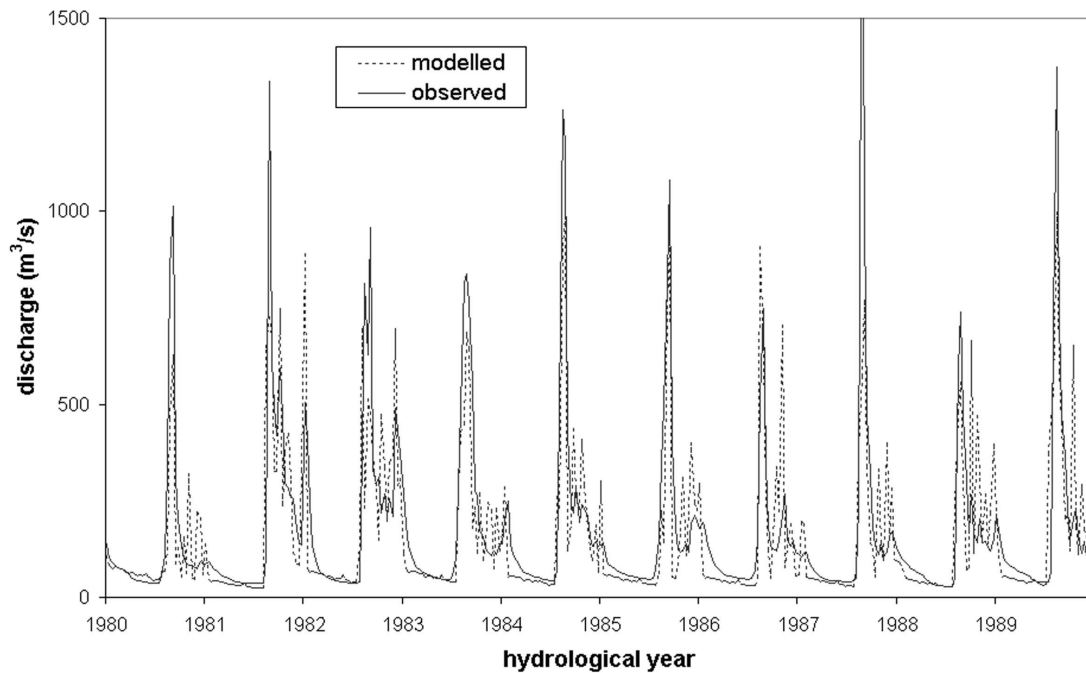


Figure 5.4 Simulated and observed discharge at Polmak, Norway, in the calibration period 1980-1989 (10-day periods). The parameter combination used here is: $DDF = 14 \text{ mm } ^\circ\text{C}^{-1} \text{ period}^{-1}$, $\chi = 0.7$, and $C = 30$ 10-day periods

It appears that the modelling efficiency, as described by the Nash-Sutcliffe coefficient, is least influenced by the recession parameter, and most by the degree-day factor. If the DDF was too low, say less than $10 \text{ mm} \cdot ^\circ\text{C}^{-1} \cdot \text{period}^{-1}$, the simulated snowmelt discharge peaks were too late and too low, compared with the observed ones. Similarly, if the DDF was $20 \text{ mm} \cdot ^\circ\text{C}^{-1} \cdot \text{period}^{-1}$ or higher, the discharge peaks at Polmak were sometimes simulated too early. For good results a DDF in the range of $10\text{-}20 \text{ mm} \cdot ^\circ\text{C}^{-1} \cdot \text{period}^{-1}$ had to be accompanied by a high separation ratio of $0.6\text{-}0.8$; with lower values of χ the simulated peak discharges were too low. Apparently the DDF is of particular importance for determining the timing of the snowmelt peak, and χ for adjusting the height of the peak discharge, although it can be seen in figure 5.4 that the runoff peaks are still too low in general.

At the same time the recession parameter primarily controls the shape - and more specifically the slope - of the recession limb of the hydrograph during winter. The higher the value for C , the more horizontal the recession curve will be, simply because the drainage of the groundwater reservoir is slower. A value of 10 periods of ten days for C gave the best results. Correct simulation of the recession limb is however not only dependent on C , but also on χ . The separation ratio determines how much water will drain to the groundwater reservoir, and in consequence the position of the simulated recession curve above or below the observed discharge. In general, a χ of $0.3\text{-}0.5$ resulted in a simulated recession limb that coincided with the observed one.

Table 5.7 Best parameter combinations in the calibration period in terms of the Nash-Sutcliffe coefficient, for the Tana River and several sub-basins. For locations, see figure 5.1

Discharge station	River	$DDF^{(a)}$	χ	$C^{(b)}$	Nash-Sutcliffe
Polmak	Tana	14	0.7	30	0.59
Alaköngäs	Tana	14	0.8	30	0.65
Onnelansuvanto	Tana	14	0.8	30	0.63
Patoniva	Utsjoki	20	0.6	20	0.63
Karigasniemi	Inarijoki	20	0.8	20	0.58
Vækkava	Jiesjåkka	14	0.6	5	0.60
Njalmigoaika	Karasjåkka	20	0.7	30	0.64

^(a) Units $\text{mm } ^\circ\text{C}^{-1} \text{ period}^{-1}$

^(b) Units 10-day periods

The Nash-Sutcliffe coefficient describes how well seasonal variations in the stream flow are simulated. When the model is calibrated on this coefficient, it is optimised to simulate the snowmelt discharge peaks. A high Nash-Sutcliffe value therefore does not necessarily mean that the performance of the model in the rest of the year is satisfying, as can be seen in figure 5.4. This diagram shows clearly that the parameter combination that gives the highest possible Nash-Sutcliffe value, results in a significant overestimation of the discharge peaks in summer, and an underestimation of the discharge in fall and winter. It seems that for the rest of the year a different parameter with lower χ values and a C of about 10 or 20 would be more appropriate.

For that reason it was decided to calculate a mean absolute bias error separately for three periods: the spring snowmelt peak (May and June), the summer period (July - September) and the winter recession period (October - April). The mean absolute bias error was also calculated for the combined summer, fall and winter period (July - April, i.e. all months except May and June). The mean absolute bias error (MABE) is similar to the mean bias error used by Barr et al. (1997), but is based on absolute differences between measured and simulated discharge. In this way periods in which the simulated runoff is higher than the observed, are not averaged out by periods in which the opposite is the case. It is calculated as follows:

$$MABE = \frac{\sum_{i=1}^k |Q_i - Q_{si}|}{\sum_{i=1}^k Q_i} \quad (5.12)$$

where Q_i = observed discharge in time period i ($\text{m}^3 \text{s}^{-1}$)
 Q_{si} = simulated discharge ($\text{m}^3 \text{s}^{-1}$)
 k = number of time steps

MABE values close to 0 indicate good agreement between measurement and simulation, while a value of 1 indicates that the total accumulative differences are equal in size to the sum of the measurements.

The smallest MABE value for the snowmelt period was obtained with a DDF of 14 $\text{mm} \cdot ^\circ\text{C}^{-1} \cdot \text{period}^{-1}$, and χ equal to 0.7 or 0.8 (see table 5.8); the value that was chosen for C had little influence on the performance of the model in May and June. For the summer period however, the best results were obtained with χ between 0.2 and 0.4, and C ranging between 30 and 40. In the winter period somewhat higher values for χ (between 0.3 and 0.5) and similar values for C (between 20 and 50) gave the lowest error values. The DDF had little influence on the model performance in both the summer and winter periods.

Figure 5.5.a shows the simulation of the parameter combination that gave the best results in the summer period. Indeed the discharge in summer is simulated well and the peaks that could be seen in figure 5.4 have disappeared. However, the snowmelt peak in spring is almost completely missed, and in winter the discharge is too high. Due to the lower separation ratio the amount of rapid runoff is lower, and more water is added to the groundwater storage, which is then drained slowly throughout the winter. The best parameter combination for the winter period is shown in figure 5.5.b. The recession limb of the annual hydrograph is now simulated very well, but the discharge peaks in summer are too high, which is caused by the higher separation ratio and more rapid groundwater drainage. Also the snowmelt peaks in spring are still too low.

In conclusion, the parameter combinations that give the best results for the summer or winter period, are different from those for the snowmelt period in spring. Only in the

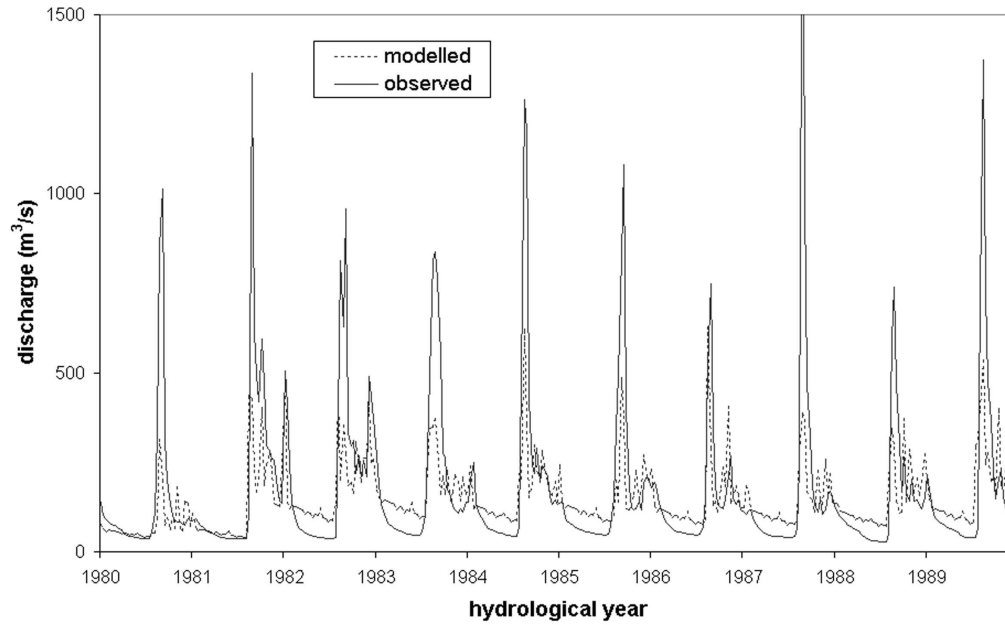
Table 5.8 Best parameter combinations at Polmak in the calibration period, in terms of the mean absolute bias error (MABE), for the spring (May and June), summer (July-September) and winter (October-April) seasons, as well as the combined summer-winter season (July-April)

Season	$DDF^{(a)}$	χ	$C^{(b)}$	MABE
Spring	14	0.8	5	0.34
Summer	20	0.3	40	0.33
Winter	14	0.5	20	0.35
Summer + winter	14	0.5	20	0.40

^(a) Units $\text{mm } ^\circ\text{C}^{-1} \text{ period}^{-1}$

^(b) Units 10-day periods

(a)



(b)

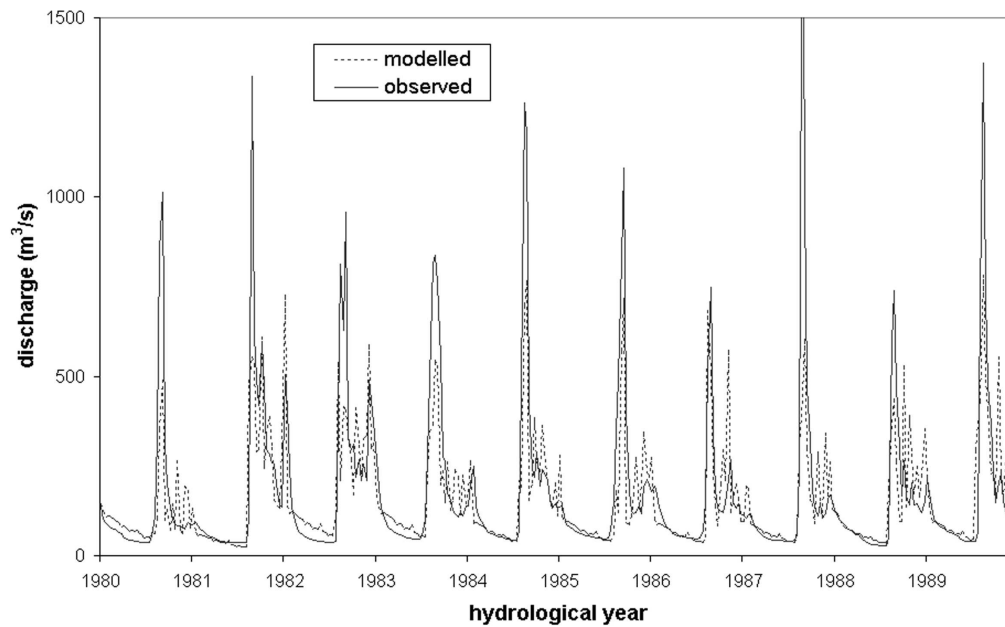


Figure 5.5 Simulated and observed discharge at Polmak, Norway, in the calibration period 1980-1989, (a) for the parameter combination $DDF = 20 \text{ mm } ^\circ\text{C}^{-1} \text{ period}^{-1}$, $\chi = 0.3$, and $C = 40$ 10-day periods, and (b) for the parameter combination $DDF = 14 \text{ mm } ^\circ\text{C}^{-1} \text{ period}^{-1}$, $\chi = 0.5$, and $C = 20$ 10-day periods.

latter case the best parameter combination was similar to what was found by calibration on the Nash-Sutcliffe coefficient. Moreover, it seems that the separation parameter χ has the largest influence on the model performance.

5.5.4 Validation

The model was validated for the period 1990-1999. Discharge measurements in Polmak stopped in 1992, and in nearby Polmak Nye in 1994 (table 5.6). The results for Alaköngäs, Finland, are summarised in table 5.9 for the three parameter combinations listed in table 5.8. In general the simulation results are better in the validation period than in the calibration period, which is probably because of the lower peak discharges (figure 5.6). At Polmak the highest Nash-Sutcliffe coefficient in the calibration period (0.59) was obtained with the parameter combination $DDF = 14$, $\chi = 0.7$ and $C = 30$. The water balance characteristics of the Tana Basin upstream of Alaköngäs for this parameter combination are summarised in table 5.10, for both the calibration and the validation period, as well as the total simulation period of 20 years (1980-1999). At Alaköngäs this combination results in a Nash-Sutcliffe coefficient of 0.63 in the calibration period, 0.71 in the validation period and 0.67 for the total period (figure 5.6). Also the parameter combinations in table 5.9 result in higher Nash-Sutcliffe coefficients and lower spring MABE values in the validation period. There is little difference in MABE values of the summer and winter periods between calibration and validation period, and sometimes the

Table 5.9 Model performance at Alaköngäs, Finland, for the calibration (1980-1989), validation (1990-1999) and total (1980-1999) simulation period, for the parameter combinations in table 5.8

Parameter combination			Period	Error statistics			
$DDF^{(a)}$	χ	$C^{(b)}$		Nash-Sutcliffe	MABE spring	MABE summer	MABE winter
14	0.8	5	1980-89	0.64	0.39	0.56	0.85
			1990-99	0.66	0.38	0.52	0.84
			1980-99	0.66	0.38	0.54	0.84
20	0.3	40	1980-89	0.39	0.64	0.29	0.61
			1990-99	0.51	0.57	0.32	0.79
			1980-99	0.44	0.61	0.30	0.70
14	0.5	20	1980-89	0.56	0.53	0.36	0.35
			1990-99	0.70	0.42	0.35	0.35
			1980-99	0.62	0.47	0.35	0.35

^(a) Units $\text{mm } ^\circ\text{C}^{-1} \text{ period}^{-1}$

^(b) Units 10-day periods

error values have even increased. This supports the idea that the improved model performance can be attributed to lower peak discharges in the validation period. In this respect it is interesting to remind that the average temperature was higher in the validation period than in the calibration period (-1.51 and -2.50°C respectively).

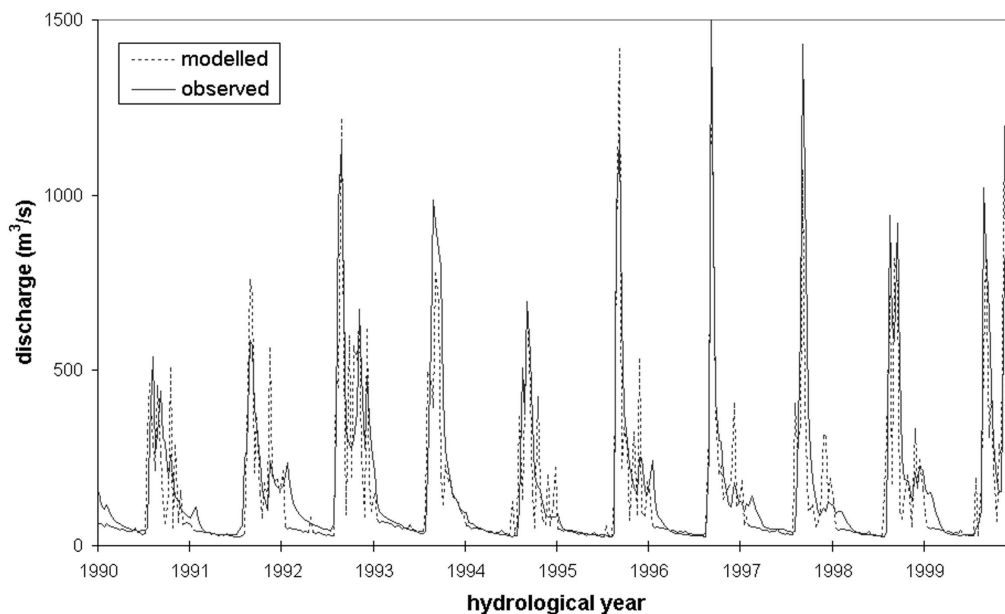


Figure 5.6 Simulated and observed discharge at Alaköngäs, Finland, in the validation period 1990-1999, for the parameter combination $DDF = 14 \text{ mm } ^{\circ}\text{C}^{-1} \text{ period}^{-1}$, $\chi = 0.7$, and $C = 30$ 10-day periods

5.6 Discussion

Although the hydrological regime of the Tana river is different from the Rhine, the model performance of TANAFLOW was similar or even somewhat better than reported by Van Deursen (1999^b). This justifies the conclusion that conceptual water balance models can successfully be applied to sub-arctic regions. Analysis and simulation of the water balance of the Tana Basin is however complicated by uncertainties about the actual amount of precipitation in the catchment. Presumably, precipitation amounts at the meteorological stations in the area, mostly located in river valleys, are significantly lower than in the surrounding uplands. As a consequence, it is not possible to derive the actual amount of evapotranspiration in the Tana Basin from the water balance. Measurements in the area suggest that total evapotranspiration in summer is much higher than the remainder of precipitation and runoff of about 3 mm/year (cf. Harding et al., 2002). The model estimate of 40 mm/year is unfortunately not based on a physical algorithm, but on the highly empirical method of Thornthwaite & Mather (1955; 1957), adjusted with an arbitrary reduction factor to meet the long-term ratio of runoff and precipitation. Realistic simulation of the water balance therefore requires better estimates of evaporation losses, either by analysis of small-scale measurements (chapter 3), or at a larger scale by using evaporation models that are more physically based (chapter 7).

Table 5.10 Water balance of the Tana Basin upstream of Alaköngäs in the simulation period (1980-1999), for the parameter combination $DDF = 14 \text{ mm } ^\circ\text{C}^{-1} \text{ period}^{-1}$, $\chi = 0.7$, and $C = 30$ 10-day periods. Explanation: Q = observed discharge, Q_s = simulated discharge, P = precipitation, E_a = actual evapotranspiration

	1980-1989	1990-1999	1980-1999
Total Q ($\times 10^{10} \text{ m}^3$)	5.9	5.6	11.5
Mean Q (m^3/s)	185.6	176.3	182.1
Total Q_s ($\times 10^{10} \text{ m}^3$)	4.8	4.9	9.6
Mean Q_s (m^3/s)	150.3	152.9	151.6
$Q - Q_s$ (mm/year)	83.9	55.4	69.6
Q/P ratio	1.10	1.03	1.06
Q_s/P ratio	0.89	0.89	0.89
$(Q_s + E_a)/P$ ratio	0.99	0.99	0.99
Mean E_a (mm/year)	40.4	39.8	40.1

Since all precipitation in the winter months accumulates as snow, the uncertainties about the actual amounts of precipitation also affect the simulation of the spring discharge peak resulting from snowmelt. As a consequence, TANAFLOW had in particular difficulties in accurately simulating the height of the peak runoff. For this reason the model performed better in the validation period, when peak discharges were generally lower than in the calibration period. Moreover, in TANAFLOW snow accumulation and snowmelt are simulated using a temperature-index approach, which is essentially a black box model as well. Although practical and straightforward, it lacks a sufficient physical basis for applications such as predicting the spatial distribution of melt in heterogeneous terrain, or transferring the model to different climatic conditions (Williams & Tarboton, 1999). Especially in climate change studies it would be better to use an energy balance model, that is applicable to a wide range of climatic conditions, and independent of calibration (see chapter 7). In the present study, the degree-day factor (DDF) was obtained by calibrating the model on river discharge data. However, this does not necessarily imply that the model is able to simulate spatial patterns in snow coverage realistically. In chapter 6, the spatial model performance is therefore tested by comparing the simulations with remotely sensed observations on snow cover depletion.

The Nash & Sutcliffe (1970) criterion that is widely used to the performance of hydrological models, is particularly sensitive to peak discharges, that dominate the hydrograph of sub-arctic rivers. However, a high efficiency coefficient does not mean that the simulation is acceptable throughout the year. In the present study, it appeared useful to calculate several error statistics, such as the mean absolute bias error (MABE) (equation 5.12), for different seasons. In this way, the performance of the model in the summer and winter periods could be evaluated. The different optimal parameter combinations that were found in this way correspond to the distinct hydrological regime

of sub-arctic environments. All precipitation falling in winter is accumulated in the snow pack, although sublimation can be significant for blowing snow, or snow intercepted on a forest canopy (Pomeroy & Gray, 1995; Lundberg et al., 1998). In spring this volume of water is released within a short period of time. Since infiltration and storage of meltwater may be limited by ice horizons in the snow pack and by frozen soils, most of it will contribute to rapid runoff. In the Tana Basin, as much as 65 % of the total annual runoff may be discharged in the spring months April to June. Later in summer, when the soil has thawed and an active layer has formed, storage of water in the soil becomes more important. In this season evapotranspiration can also be significant. As a consequence, rapid runoff will be much less important, except maybe for extreme rainfall events. In winter, discharge is very low and consists primarily of baseflow. Currently, not all of these processes are properly represented in TANAFLOW. For example, during winter and spring there is no constraint on infiltration, that would account for underlying snow layers and frozen soils. This explains why the best results in the spring period were obtained with a high value for the separation ratio (χ), while in summer a lower value performed better. By introducing a conceptual representation of soil frost in the model, it may be possible to simulate the hydrological behaviour of the Tana Basin more realistically.

5.7 Conclusions

In this study it was demonstrated that a conceptual water balance, originally developed for the Rhine, can successfully be applied to the sub-arctic Tana River Basin. However, before such a model can be used in hydrological impact studies of climate change in sub-arctic environments, several issues may need to be improved. First of all, the simulations were complicated by uncertainties about the actual amount of precipitation over the catchment. As a result, the actual amount of evapotranspiration cannot be derived from the water balance, nor can it safely be deduced from the empirical algorithm that is currently employed in the model. Secondly, snowmelt in spring, that dominates the hydrological regime of the Tana River, is simulated by using a highly empirical method as well. Since the temperature-index model is calibrated on river runoff, it remains uncertain whether it is able to simulate spatial patterns in snow coverage realistically. Finally, it may be necessary to include a representation of soil frost in the model, in order to take account of the differences in hydrological behaviour between winter, spring and summer. In chapter 7, physically-based algorithms for snowmelt and evapotranspiration, will be introduced into TANAFLOW, in combination with a conceptual representation of the effect of frozen soils on the infiltration during snowmelt. Before that, the simulation of spatial patterns in snow cover depletion is evaluated in chapter 6, and a first assessment is made of the sensitivity of snow cover dynamics to changes in climate.

5.8 References

Addiscott, T., J. Smith & N. Bradbury (1995): Critical evaluation of models and their parameters. *Journal of Environmental Quality* 24, pp. 803-807.

- Arnell, N. (1999): A simple water balance model for the simulation of streamflow over a large geographic domain. *Journal of Hydrology* 217, pp. 314-335.
- Barr, A.G., G.W. Kite, R. Granger & C. Smith (1997): Evaluating three evapotranspiration methods in the SLURP macroscale hydrological model. *Hydrological Processes* 11, pp. 1685-1705.
- Bouwman, A.F., I. Fung, E. Matthews & J. John (1993): Global analysis of the potential for nitrous oxide (N₂O) production in natural soils. *Global Biogeochemical Cycles* 7, pp. 557-597.
- Bergström, S. (1995): The HBV model. In: V.P. Singh (ed.): *Computer Models of Watershed Hydrology*. Highlands Ranch, Colorado: Water Resources Publications, pp. 443-476.
- Brechtel, H.M. & G. Scheele (1982): *Erwirtschaftung von Grundwasser durch Land- und Forstwirtschaftliche Massnahmen*. Hannover: Hessische Forstliche Versuchsanstalt.
- Defense Mapping Agency (1986): *Defense Mapping Agency product specifications for digital terrain elevation data (DTED)*. St. Louis: Defense Mapping Agency Aerospace Center.
- Ferguson, R.I. (1999): Snowmelt runoff models. *Progress in Physical Geography* 23, pp. 205-227.
- Harding, R.J., N.A. Jackson, E.M. Blyth & A. Culf (2002): Evaporation and energy balance of a sub-arctic hillslope in northern Finland. *Hydrological processes* 16, pp. 1419-1436.
- Goodison, B.E., P.Y.T. Louie & D. Yang (1998): *WMO solid precipitation measurement intercomparison, final report*. Geneva: World Meteorological Organization (WMO Instruments and Observing Methods Report No. 67, WMO/TD-No.872).
- Groenendijk, H. (1989): *Estimation of waterholding-capacity of soils in Europe: the compilation of a soil dataset*. Wageningen: Centre for Agrobiological Research, Department of Theoretical Production Ecology, Agricultural University (Simulation reports CABO-TT 19).
- Kite, G.W. (1995): The SLURP model. In: V.P. Singh (ed.): *Computer Models of Watershed Hydrology*. Highlands Ranch, Colorado: Water Resources Publications, pp.521-562.
- Kite, G.W. & N. Kouwen (1992): *Watershed modelling using land classifications*. *Water Resources Research* 28, pp. 3193-3200.
- Kwadijk, J.C.J. (1993): *The impact of climate change on the discharge of the River Rhine*. Utrecht: Koninklijk Aardrijkskundig Genootschap / Faculteit Ruimtelijke Wetenschappen Universiteit Utrecht (Netherlands Geographical Studies 171).
- Lammi, J. (2001): *Online photoperiod calculator and sunrise / sunset calculator for MS Excel*. Available from <http://www.nic.fi/~benefon/sun.php3>, accessed on 30 July 2002.
- Lindström, G., B. Johansson, M. Persson, M. Gardelin & S. Bergström (1997): Development and test of the distributed HBV-96 model. *Journal of Hydrology* 201, pp. 272-288.
- Lundberg, A., I. Calder & R.J. Harding (1998): Evaporation of intercepted snow: measurement and modelling. *Journal of Hydrology* 206, pp. 151-163.
- Mackay, D.K. & O.H. Løken (1974): *Arctic Hydrology*. In: J.D. Ives & R.G. Barry (eds.): *Arctic and Alpine Environments*. London: Methuen, pp. 111-132.
- Martinez, J., A. Rango & R. Roberts (1994): *Snowmelt runoff model (SRM) user's manual* (M.F. Baumgartner, ed.) Bern: Department of Geography, University of Bern (Geographica Bernensia P29).
- Melloh, R.A. (1999): *A synopsis and comparison of selected snowmelt algorithms*. Hanover, New Hampshire: US Army Corps of Engineers, Cold Regions Research & Engineering Laboratory (CCREL report 99-8).
- Milly, P.C.D. (1994): Climate, interseasonal storage of soil water, and the annual water balance. *Advances in Water Resources* 17, pp. 19-24.
- Nash, J.E. & Sutcliffe, J.V. (1970): River flow forecasting through conceptual models; Part 1 -a discussion of principles. *Journal of Hydrology* 10, pp. 282-290.
- Olsen, L., A. Reite, K. Riibe & E. Sørensen (1996): *Finnmark county, Map of Quaternary Geology, scale 1:500,000, with description*. Trondheim: Geological Survey of Norway.
- Penman, H.L. (1956): *Evaporation: an introductory survey*. *Netherlands Journal of Agricultural Science* 4, pp. 9-29.
- Pereira, A.R. & A.P. Camargo (1989): An analysis of the criticisms of Thornthwaite's equation for estimating potential evapotranspiration. *Agricultural and Forest Meteorology* 46, pp. 149-157.
- Pomeroy, J.W. & D.M. Gray (1995): *Snow cover accumulation, relocation and management*. Saskatoon: National Hydrology Research Institute (NHRI Science Report 7).

- Quinton, W.L. & N.T. Roulet (1998): Spring and summer runoff hydrology of a subarctic patterned wetland. *Arctic and Alpine Research* 30, pp. 285-294.
- Rosenberg, N.J., B.L. Blad & S.B. Verma (1983): *Microclimate, The Biological Environment*. New York: Wiley.
- Rovanssek, R.J., L.D. Hinzman & D.L. Kane, D.L. (1996): Hydrology of a tundra wetland complex on the Alaskan Arctic Coastal Plain, U.S.A. *Arctic and Alpine Research* 28, pp. 311-317.
- Sellinger, C.E. (1996): Computer program for estimating evapotranspiration using the Thornthwaite method. Ann Arbor, Michigan: National Oceanic and Atmospheric Administration (NOAA), Great Lakes Environmental Research Laboratory (NOAA Technical Memorandum ERL GLERL-101).
- Shuttleworth, W.J. (1993): Evaporation. In: D.R. Maidment (ed.): *Handbook of Hydrology*. New York: McGraw-Hill, pp. 4.1-4.53.
- Singh, P., N. Kumar & M. Arora (2000): Degree-day factors for snow and ice for the Dokriani Glacier, Garhwal Himalayas. *Journal of Hydrology* 235, pp. 1-11.
- Thornthwaite, C.W. & J.R. Mather (1955): *The water balance*. Centerton: Drexel Institute of Technology, Laboratory of Climatology (Publications in Climatology 8).
- Thornthwaite, C.W. & Mather, J.R. (1957): Instructions and tables for computing potential evapotranspiration and the water balance. Centerton: Drexel Institute of Technology, Laboratory of Climatology (Publications in Climatology 10), pp. 183-243.
- United States Geological Survey (USGS) (2002): GTOPO30 documentation. Available from <http://edcdaac.usgs.gov/gtopo30/README.html>, accessed on 30 July 2002.
- Van der Wateren – de Hoog, B. (1997): Quantification of catchment discharge sensitivity to climate variability. Utrecht: Koninklijk Aardrijkskundig Genootschap / Faculteit Ruimtelijke Wetenschappen Universiteit Utrecht (Netherlands Geographical Studies 233).
- Van Deursen, W.P.A. (1995): *Geographical Information Systems and Dynamic Models. Development and application of a prototype spatial modelling language*. Utrecht: Koninklijk Aardrijkskundig Genootschap / Faculteit Ruimtelijke Wetenschappen Universiteit Utrecht (Netherlands Geographical Studies 190).
- Van Deursen, W.P.A. (1999^a): RHINEFLOW-2: Development, calibration and application. Rotterdam: Carthago Consultancy (report of the NRP project 952210).
- Van Deursen, W.P.A. (1999^b): Impact of climate change on the river Rhine discharge regime. Rotterdam: Carthago Consultancy (report of the NRP project 952210).
- Vörösmarty, C.J., B. Moore, M.P. Gildea, B. Peterson, J. Melillo, D. Kicklighter, J. Raich, E. Rastetter & P. Steudler (1989): A continental-scale model of water balance and fluvial transport: application to South America. *Global Biogeochemical Cycles* 3, pp. 241-265.
- Ward, R.C. & M. Robinson (1990): *Principles of Hydrology*. London: McGraw-Hill.
- Wesseling, C.G., W.P.A. Van Deursen & M. De Wit, M. (1997): Large scale catchment delineation: a case study for the River Rhine basin. In: S. Hodgson, M. Rumor & J.J. Harts (eds.): *Geographical Information '97 (Third Joint European Conference & Exhibition on Geographical Information, Vienna, Austria)*, pp. 487-496.
- Williams, K.S. & D.G. Tarboton (1999): The ABC's of snowmelt: a topographically factorized energy component snowmelt model. *Hydrological Processes* 13, pp. 1905-1920.
- Woo M.-K. (1990): Permafrost Hydrology. In: T.D. Prowse & C.S.I. Ommanney (eds.): *Northern Hydrology, Canadian Perspectives*. Saskatoon: National Hydrology Research Institute (NHRI Science Report 1), pp. 63-76.
- Xu, C.-Y. (1999): From GCMs to river flow: a review of downscaling methods and hydrologic modelling approaches. *Progress in Physical Geography* 23, pp. 229-249.
- Yang, D. & M.-K. Woo (1999): Representativeness of local snow data for large scale hydrologic investigations. *Hydrological Processes* 13, pp. 1977-1988.
- Yang, D., B.E. Goodison, J.R. Metcalfe, P.Y.T. Louie, E. Elomaa, C.L. Hanson, V.S. Golubev, Th. Gunther, J. Milkovic & M. Lapin (2001): Compatibility evaluation of national precipitation gauge measurements. *Journal of Geophysical Research* 106, pp. 1481-1492.
- Zobler, L.(1986): *A world soil file for global climate modelling*. New York: NASA Goddard Institute for Space Studies (NASA Technical Memorandum 87802).